ORNL/TM-2024/3350

# Oak Ridge National Laboratory

# Scoping Studies on the Impacts of Increased Enrichment on Nuclear Criticality Safety


Alex M. Shaw
Walid A. Metwally
William J. Marshall

**May 2024**

OAK RIDGE National Laboratory

ORNL IS MANAGED BY UT-BATTELLE LLC FOR THE US DEPARTMENT OF ENERGY

## DOCUMENT AVAILABILITY

Reports produced after January 1, 1996, are generally available free via OSTI.GOV.

***Website*** www.osti.gov

Reports produced before January 1, 1996, may be purchased by members of the public from the following source:

National Technical Information Service
5285 Port Royal Road
Springfield, VA 22161
***Telephone*** 703-605-6000 (1-800-553-6847)
***TDD*** 703-487-4639
***Fax*** 703-605-6900
***E-mail*** info@ntis.gov
***Website*** http://classic.ntis.gov/

Reports are available to US Department of Energy (DOE) employees, DOE contractors, Energy Technology Data Exchange representatives, and International Nuclear Information System representatives from the following source:

Office of Scientific and Technical Information
PO Box 62
Oak Ridge, TN 37831
***Telephone*** 865-576-8401
***Fax*** 865-576-5728
***E-mail*** reports@osti.gov
***Website*** https://www.osti.gov/

**ORNL/TM-2024/3350**

Nuclear Energy and Fuel Cycle Division

# SCOPING STUDIES ON THE IMPACTS OF INCREASED ENRICHMENT ON NUCLEAR CRITICALITY SAFETY

Alex M. Shaw
Walid A. Metwally
William J. Marshall

May 2024

Prepared by
OAK RIDGE NATIONAL LABORATORY
Oak Ridge, TN 37831
managed by
UT-BATTELLE LLC
for the
US DEPARTMENT OF ENERGY
under contract DE-AC05-00OR22725

**CONTENTS**

CONTENTS ..... iii
LIST OF FIGURES ..... iv
LIST OF TABLES ..... v
ABBREVIATIONS ..... vi
ABSTRACT ..... 1
1. Introduction ..... 1
2. Case Studies ..... 1
    2.1 CASE I: Single-assembly Scoping Study ..... 2
    2.2 CASE II: Single-assembly Full Study ..... 2
3. Computational Methods and Models ..... 3
4. Results and Discussion ..... 9
    4.1 Case I: Single-assembly Scoping Study ..... 9
    4.2 CASE II: Single-assembly Full Study ..... 12
5. Conclusions ..... 17
6. References ..... 18

## LIST OF FIGURES

Figure 3-1. IFBA (yellow) loading patterns, clockwise from top left: 80 IFBA, 128 IFBA, 200 IFBA, and 220 IFBA. ..... 4
Figure 3-2. Gadolinium-bearing rods (red) inserted into an 128 IFBA-bearing (yellow) PWR array under (a) reference loading and (b) adjusted loading. ..... 5
Figure 3-3. BWR lattice with 20 gadolinium bearing rods shown in red. ..... 6
Figure 3-4. 3D Models of (a) PWR lattice with 220 IFBA and (b) BWR lattice with 20 Gd rods. ..... 7
Figure 3-5. Vanished lattice of BWR assembly. ..... 8
Figure 3-6. Gadolinium bearing rod (red) placement in a BWR assembly. Listed clockwise; Edge, Corner Oblong, Cluster, Corner. ..... 8
Figure 3-7. Concrete (grey) reflection on four sides of a BWR assembly. ..... 9
Figure 4-1. $k_{eff}$ at different IFBA loadings for a PWR assembly at 10 wt % $^{235}U$. ..... 10
Figure 4-2. $k_{eff}$ at different IFBA loading patterns and gadolinium loadings for a PWR assembly at 15 wt % $^{235}U$. ..... 10
Figure 4-3. $k_{eff}$ at different IFBA loading patterns and gadolinium loadings for a PWR assembly at 20 wt % $^{235}U$. ..... 11
Figure 4-4. $k_{eff}$ at different fuel enrichments and gadolinium loadings for a BWR assembly with 20 gadolinium bearing rods. ..... 12
Figure 4-5. Summary of burnable absorber and fuel enrichment requirements for Case I. ..... 12
Figure 4-6. $k_{eff}$ differential for Cr-Coated PWR fuel by IFBA and enrichment. ..... 13
Figure 4-7. $k_{eff}$ differential for Cr-Coated BWR fuel. ..... 14
Figure 4-8. $k_{eff}$ differential for $Cr_2O_3$-doped PWR fuel by IFBA and enrichment. ..... 14
Figure 4-9. $k_{eff}$ differential for $Cr_2O_3$-doped BWR fuel. ..... 15
Figure 4-10. $k_{eff}$ differential for PWR concrete reflection. ..... 16
Figure 4-11. $k_{eff}$ differential for BWR concrete reflection. ..... 16

## LIST OF TABLES

Table 1. Variables considered in the single-assembly scoping study ..... 2
Table 2. PWR nominal assembly geometric parameters [14] ..... 3
Table 3. BWR nominal assembly geometric parameters [9] ..... 5
Table 4. Calculated $k_{eff}$ for ATF concepts ..... 13
Table 5. Calculated $k_{eff}$ for BWR gadolinium rod placement ..... 15
Table 6. Calculated $k_{eff}$ for PWR annular blanket ..... 15

## ABBREVIATIONS

| | |
|---|---|
| ATF | accident-tolerant fuel |
| BWR | boiling water reactor |
| CFR | US Code of Federal Regulations |
| ENDF | Evaluated Nuclear Data File |
| HALEU | high-assay low-enriched uranium |
| IE | increased enrichment |
| IFBA | integral fuel burnable absorber |
| ORNL | Oak Ridge National Laboratory |
| PWR | pressurized water reactor |

## ABSTRACT

Fuel vendors and industry are increasingly interested in new fuel designs with increased enrichment. These fuel types are categorized as high-assay low-enriched uranium: their fuel enrichment is low in the regulatory sense, but it is much higher than industry's typical operating enrichment bounds. It should be demonstrated that the appropriate mechanisms have been established to control this increased reactivity, and the conditions that arise from common operational occurrences must be considered. This report presents case studies that were conducted to determine whether increased burnable absorber loading can be used to offset increased enrichment. Increases in integral fuel burnable absorber and gadolinium-bearing rods in pressurized water reactor (PWR) and boiling water reactor (BWR) assemblies must be examined. Increases in reactivity were shown to be feasibly controlled by increased burnable absorber loading, even when operational specificities were considered, as in BWR partial length rods and PWR annular fuel blankets.


## 1. INTRODUCTION

10 CFR 50.68 [1], Criticality Accident Requirements, specifies the criticality accident requirements with which licensees must comply. The recent interest in increased enrichment (IE) and high-assay low-enriched uranium (HALEU) fuel, specifically in the range of 10–20 wt% $^{235}U$, has prompted questions regarding the effect of this fuel on the nuclear fuel storage conditions and the degree to which the fuel meets the k-effective ($k_{eff}$) limits specified in 10 CFR 50.68. The studies described herein include an analysis of these effects for different fuel configurations.

The first case study performed was a single PWR and BWR assembly scoping study and is presented in Section 2.1. Here, eigenvalues were calculated for an individual assembly and were modeled with water reflection in an infinite array of like assemblies. The effects of enrichment and burnable absorbers were tested to demonstrate the point at which an individual assembly was considered subcritical, meeting the 0.95 $k_{eff}$ requirement specified 10 CFR 50.68, with an additional 1% of penalty added to calculated values to represent biases and uncertainties. Gadolinium bearing rods and $ZrB_2$ coated integral fuel burnable absorber (IFBA) rods were burnable absorbers used to control reactivity and power peaking.

The second case study, detailed in Section 2.2, expanded the scope of the first study, investigating the same assemblies with additional perturbations to more accurately reflect considerations in operation. For example, instead of placing the assemblies in a pool of water alone, additional concrete reflection was included to represent placement of an assembly in a fuel channel or at the edge of a fuel pool. Subtleties of reactor design such as partial length fuel rods for BWRs, annular fuel pellet blankets for PWRs, and hypothetical advanced fuel designs such as chromium coatings were also examined for their effects on criticality [2-4].

Section 3 presents the models derived in this work, along with some of the motivations, limitations, and choices made in modeling. Section 4 presents the results of the case studies and associated observations. Section 5 provides concluding remarks for the overall study.

## 2. CASE STUDIES

The work was divided into two stages, as described below.

## 2.1 CASE I: SINGLE-ASSEMBLY SCOPING STUDY

The single-assembly scoping study included PWR and BWR fuels. Information about the fuels and variables considered in this study are shown in Table 1. The same lattice is used for all PWR calculations and for all BWR calculations, with changes made to respective enrichments and amounts of burnable absorbers—$Gd_2O_3$ and IFBA rods—present in the assembly. The single assembly was modeled with water reflection in an infinite array.

**Table 1. Variables considered in the single-assembly scoping study**

| Variable | PWR | BWR |
|---|---|---|
| Lattice | 17 × 17 | 10 × 10 |
| Enrichment variants | 10, 15, 20 wt % $^{235}U$ (Uniform across the lattice) | |
| Surrounding water | 40 cm on all sides with reflective boundary conditions | |
| $Gd_2O_3$ rods | 12 (if needed) | 20 |
| $Gd_2O_3$ loading variants | 2, 4, 6, 8 wt % Gd | |
| IFBA rod variants | 80, 128, 200 | N/A |
| IFBA loading | 3.137 (2×) mg $^{10}B$/in. | N/A |

## 2.2 CASE II: SINGLE-ASSEMBLY FULL STUDY

Fuel compositions and dimensions are preserved between the scoping analysis (Case I) and the full study (Case II). Additional perturbations were performed for the full study: none involved variation of overall lattice size, enrichment, or $Gd_2O_3$ and IFBA compositions. The following studies were performed:

- Analysis of sensitivity to accident-tolerant fuel (ATF) concepts: Cr-coated cladding and Cr-doped fuel
- Analysis of sensitivity of bounding Gd-doped locations in the BWR lattice
- Investigation of the effect of PWR annular fuel blankets
- Investigation of the effect of BWR partial length rods in the vanished region
- Analysis of sensitivity of BWR/PWR assemblies to concrete reflection

As in previous work [2], a 20 μm chromium coating was applied to the fuel and to the guide cladding. This value was selected as a reasonable estimate of the potential industry design choice based on a literature search [5]. Similarly, insight provided from the Westinghouse ADOPT program indicated that a chromium oxide ($Cr_2O_3$) dopant of 1,000 ppm is reasonable. Thus, 680 ppm Cr and 320 ppm O by weight were introduced to the fuel. Fuel dopant as an ATF concept is applied to achieve, in part, a higher fuel density. Thus the densities of BWR and PWR fuel with dopant were increased by 2% of $UO_2$ theoretical density. This is a reasonable and conservative assumption, because $Cr_2O_3$ dopant, including that included in ADOPT fuel, has been shown to have a negligible to ~1.5 % increase in the theoretical density of fuel pellets [6,7]. BWR densities were increased to 10.769 g/cm$^3$, and PWR densities were increased to 10.595 g/cm$^3$.

Several gadolinium rod locations were considered using 20 wt% $^{235}U$ fuel and 2 wt% natural gadolinium. Options included clustering of gadolinium rods, placement of rods along the periphery of the assembly, and placement of rods in the corners. These placement options are not intended to be real or anticipated loading patterns for the gadolinium, but instead are being used to gauge variability caused by gadolinium placement.

To analyze PWR annular fuel blankets, 8-inch blankets were implemented at the ends of the fuel rods. This required replacement of fuel rod tips; it did not involve including an additional region of fuel.

Annular fuel blankets are applied to reduce axial leakage and accommodate fission gas release. The inner radius of the annulus was approximately half the outer radius of the pin at 0.2096 cm. The blanket enrichments considered were 2 wt% below the nominal enrichments used: 8, 13, and 18 wt% $^{235}U$.

Fourteen partial length rods were investigated in the BWR lattice. Partial length fuel rods are applied to increase the moderator to fuel ratio in the upper portion of the core to offset lower moderator densities in BWRs. Although they were not an exact match, positioning of the dominant and vanished regions was inspired by a lattice published by Fensin, as well as recent studies conducted by Oak Ridge National Laboratory (ORNL) [8,9]. The additional gadolinium-bearing rods in these lattices necessitated adjustments to the layouts in these sources with no vanished positions maintained on the assembly periphery and with vanished positions maintained near water channels and gadolinium rods. The dominant region was approximately 66% of the full height of the full rod at 252 cm tall. The cases used 20 Gd rods at 8 wt%.

A study on concrete reflection was performed to determine the effect of concrete positioned on multiple sides of an assembly. The concrete modeled is the *reg-concrete* included in the SCALE Standard Composition [10]. A 10 cm gap of water between the assembly and concrete was maintained, with 30 cm of concrete sequentially added to each radial face of the assembly. Multiple sides were modeled to determine the effect of increasing concrete reflection and to address multiple scenarios that assemblies might encounter. For instance, a single face of concrete represents an assembly resting by a wall, and two perpendicular faces of concrete represent an assembly by a wall corner. Modeling a PWR assembly surrounded on all sides by water and concrete results in a 16-inch square channel of water and concrete surrounding the assembly. For BWRs, this results in a 13-inch channel. For fuel transfer channels in PWRs, example channel inner dimensions were found to be 20 and 30 inches [11,12].

## 3. COMPUTATIONAL METHODS AND MODELS

The SCALE 6.3.1 code package with the Evaluated Nuclear Data File (ENDF/B)-VII.1 continuous energy cross sections was used in this work [10,13]. The CSAS5 sequence was used for automated data processing and neutron transport within SCALE, combining the KENO V.a Monte Carlo transport code with XSPROC nuclear data processing into an efficient, easy-to-use control module. CSAS5 models were developed for representative Westinghouse 17 × 17 PWR and GE 10 × 10 BWR lattices. The PWR and BWR geometries and lattice designs were obtained from Hu et al. [14] and Mertyurek et al. [9], respectively. The fuel assemblies are modeled with 40 cm of water on each side, with reflective boundary conditions forming an infinite array. Three $^{235}U$ enrichments were examined: 10, 15, and 20 wt %.

PWR fuel rods have a density of 10.376 g/cm$^3$, representing ~95% of the theoretical density of $UO_2$. The cladding and thimbles were composed of Zircaloy-4, which is representative of modern PWR fuel. The PWR assembly parameters are presented in Table 2.

**Table 2. PWR nominal assembly geometric parameters [14]**

| Specification | Value (cm) |
|---|---|
| Fuel radius | 0.4096 |
| Gap radius (clad inner radius) | 0.418 |
| Clad outer radius | 0.475 |
| Guide tube inner radius | 0.5715 |
| Guide tube outer radius | 0.61214 |
| Fuel rod/guide tube pitch | 1.260 |
| Fuel rod/guide tube height | 365.76 |

PWR lattices utilized IFBA rods with 80 $ZrB_2$-coated fuel rods with a boron loading of 3.137 mg $^{10}B$/in. per rod. IFBA rods have a thin deposition coating of $ZrB_2$ neutron absorber that is applied directly to fuel pellets to offset initial assembly reactivity. The IFBA locations within the assembly are selected to manage power peaking. The thin layer provides strong initial absorption, but the effect diminishes as fuel is burned in tandem with decreased fuel reactivity. IFBA patterns are selected based on the individual need for each reactor's operation and its specific goals. Three of the IFBA loading patterns in this work were drawn from Hu et al. [14], 80, 128, and 200. An additional 220 IFBA pattern was considered based on the 200 IFBA pattern, adding 20 coated rods symmetrically about the assembly. The layouts for these patterns are shown in Figure 3-1.

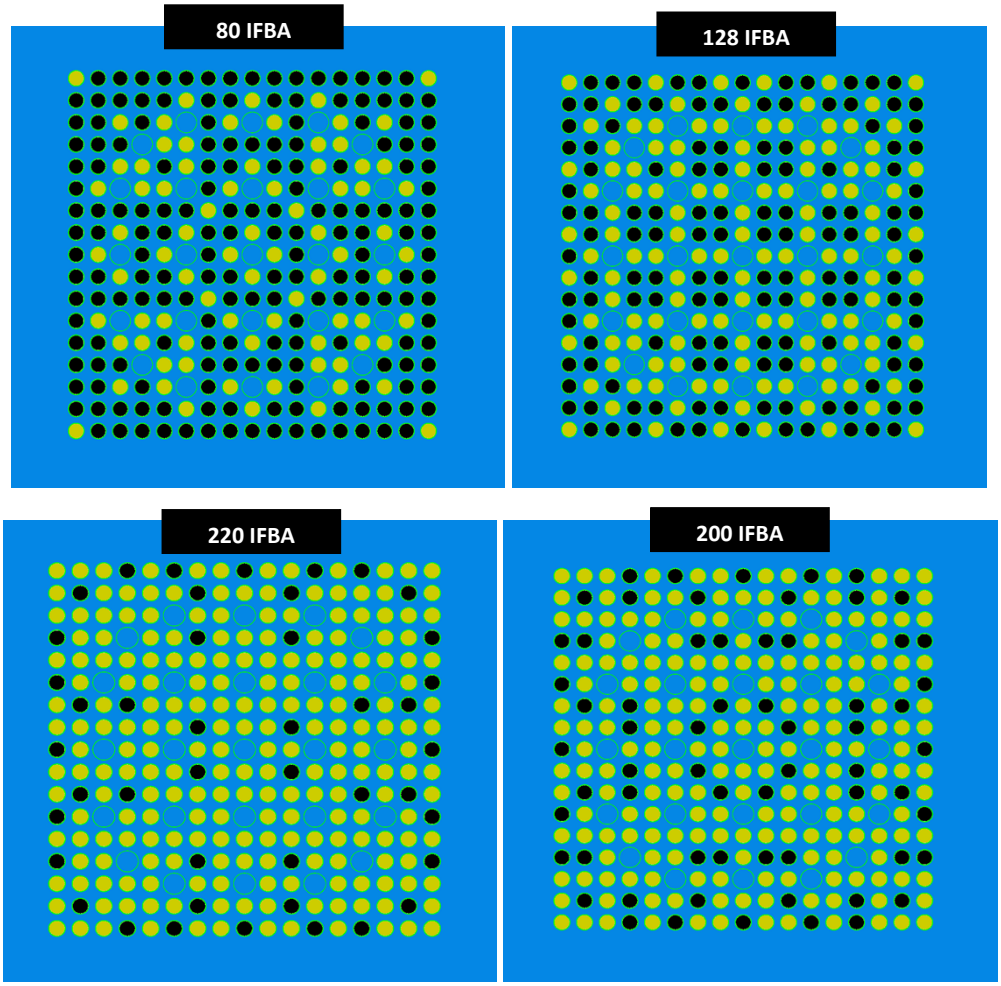


**Figure 3-1. IFBA (yellow) loading patterns, clockwise from top left: 80 IFBA, 128 IFBA, 200 IFBA, and 220 IFBA.**

In some PWR lattices, 12 additional gadolinium-bearing rods were added as an alternative to the continued increased IFBA loading. Gadolinium is used to offset initial reactivity and control power peaking in some PWRs and all BWRs. With increased enrichment, it may be necessary and efficient to offset additional initial reactivity. Although this approach was inspired by CASL-U-2012-0131-004 [15], the gadolinium rod layout had several overlapping locations with the IFBA patterns. Therefore, adjustments were made to preserve the IFBA loading and to understand the effect of adding the gadolinium rods. Figure 3-2 shows the reference gadolinium-bearing rod locations [15] and the adjusted

locations used in this study. Notably, no overlap occurs in the figure, rather demonstrating the reference and shifted positions of the Gd rods. The overlap between Gd and IFBA occurs with 80 and 200 IFBA lattice designs, for instance, the third indexed position in both directions (top to bottom, left to right). Index (3,3) contains an IFBA rod for the 80 and 200 lattice design, whereas index (2,2) does not- thus, the Gd rod was placed at index (2,2) rather than (3,3) as in the reference, to preserve the IFBA location and quantity between studies.

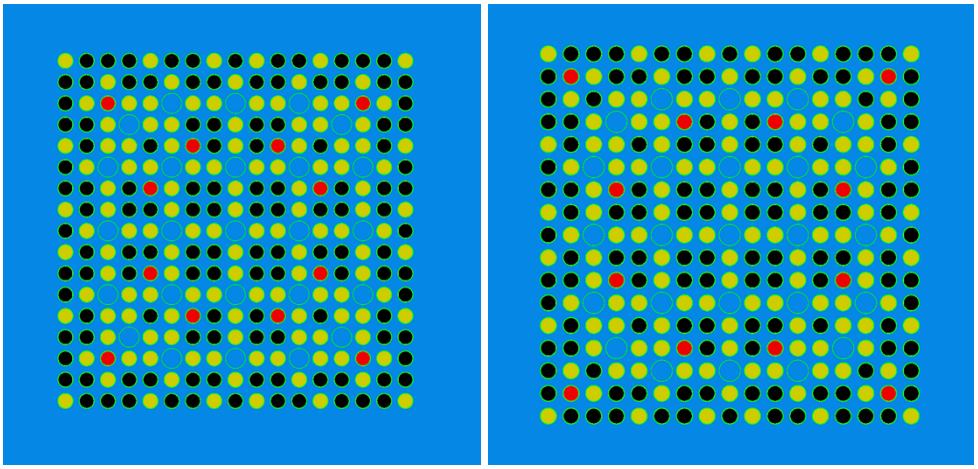

a) b)

**Figure 3-2. Gadolinium-bearing rods (red) inserted into an 128 IFBA-bearing (yellow) PWR array under (a) reference loading and (b) adjusted loading.**

Each of the gadolinium-bearing rods had an initial composition of 2 wt % $Gd_2O_3$, which was increased to 8 wt % in 2 wt % increments as needed to maintain a $k_{eff}$ below 0.94. A $k_{eff}$ of 0.94 is used to represent the 10 CFR 50.68 $k_{eff}$ limit of 0.95 including biases and uncertainties; a 0.01 margin to account for biases and uncertainties was thus applied to this work.

The 10 × 10 BWR lattices credited an initial 20 gadolinium-bearing fuel rods [14] with a composition of 2 wt % $Gd_2O_3$, increasing enrichment to 8 wt % in increments of 2 wt % as needed to maintain a $k_{eff}$ below 0.94. The fuel rods have a density of 10.550 g/cm$^3$, representing ~96% of the theoretical density of $UO_2$. The water channel and cladding are composed of Zircaloy-2, which is representative of modern BWR fuel. Table 3 includes the BWR assembly parameters, and Figure 3-3 shows the layout. The BWR assembly was modeled with full rods in the entire assembly length in Case I, with a study on partial length fuel rods in Case II.

**Table 3. BWR nominal assembly geometric parameters [9]**

| Specification | Value (cm) |
|---|---|
| Fuel radius | 0.438 |
| Gap radius (clad inner radius) | 0.447 |
| Clad outer radius | 0.513 |
| Fuel rod pitch | 1.295 |
| Fuel rod height | 381 |
| Water channel radius | 1.200 |
| Water channel thickness | 0.080 |

Figure 3-4 shows a cutaway view of the bottom halves of the PWR and BWR fuel assemblies with the water reflector. The water reflector in the figure is reduced to 10 cm and is rendered with reduced opacity, with front quarter and top half cuts for visualization.

Fifteen thousand particles per generation were simulated, with 150 generations skipped. Each case was run until an uncertainty of 10 pcm in $k_{eff}$ was reached. Appendix A includes input files for (1) a BWR assembly with 15 wt % $^{235}U$ and 20 Gd rods at 2 wt% $Gd_2O_3$ and (2) a PWR assembly with 15 wt % $^{235}U$ and 128 IFBA rods.

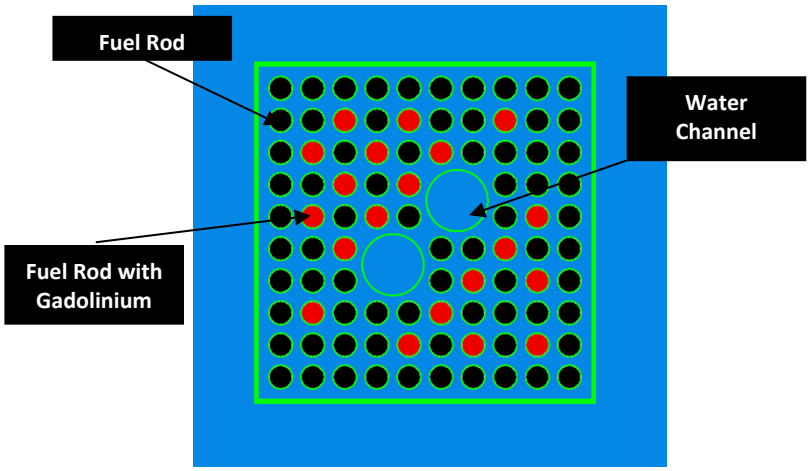


**Figure 3-3. BWR lattice with 20 gadolinium bearing rods shown in red.**

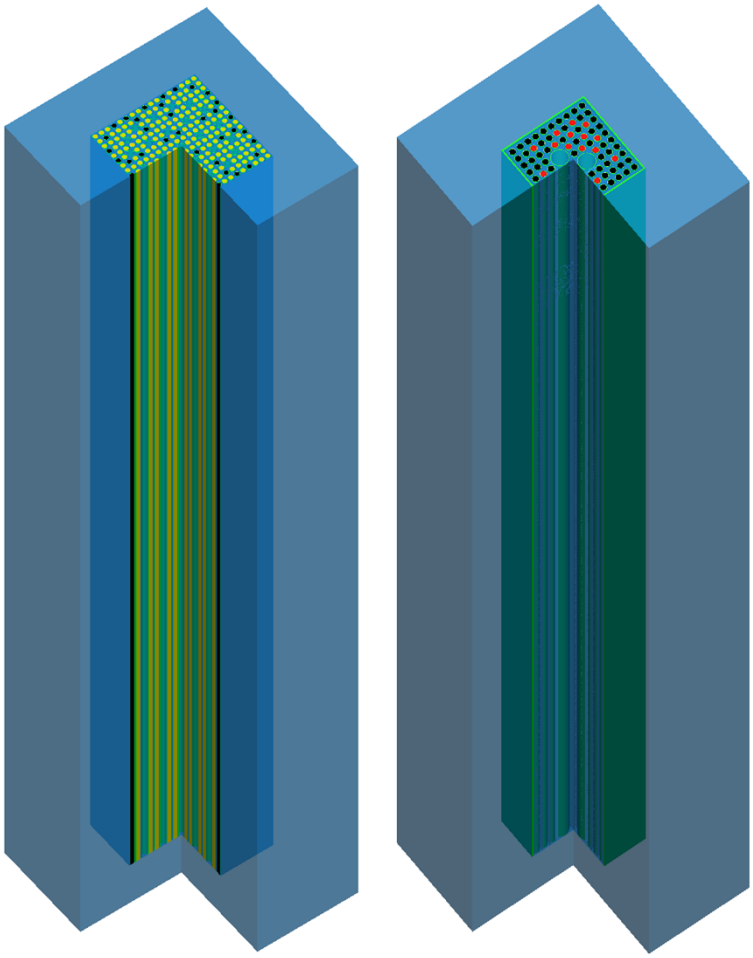

(a) (b)

**Figure 3-4. 3D Models of (a) PWR lattice with 220 IFBA and (b) BWR lattice with 20 Gd rods.**

Figure 3-5 shows the selected lattice design of the partial length study. As noted in Section 2, the 14 partial length rods were approximately ⅔ of the full-length rod height. Figure 3-6 shows the redistributed gadolinium rods used to determine the sensitivity of $k_{eff}$ to positions. Rods were placed at the periphery and in various clusters. Figure 3-7 displays where some of the water was replaced with concrete to study the effect of reflection.

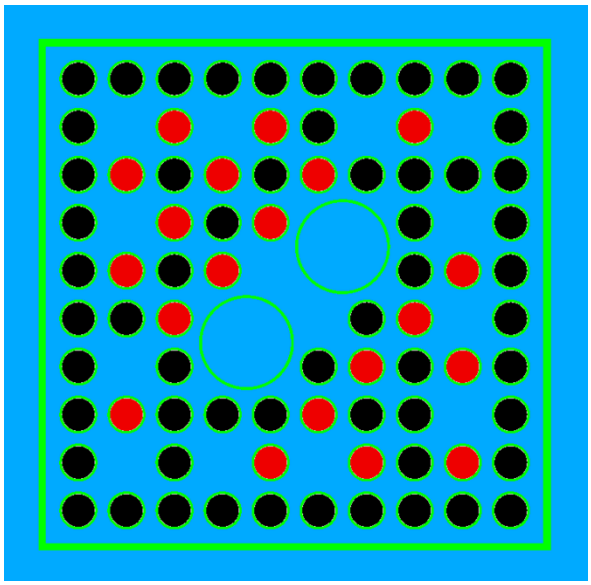

**Figure 3-5. Vanished lattice of BWR assembly.**

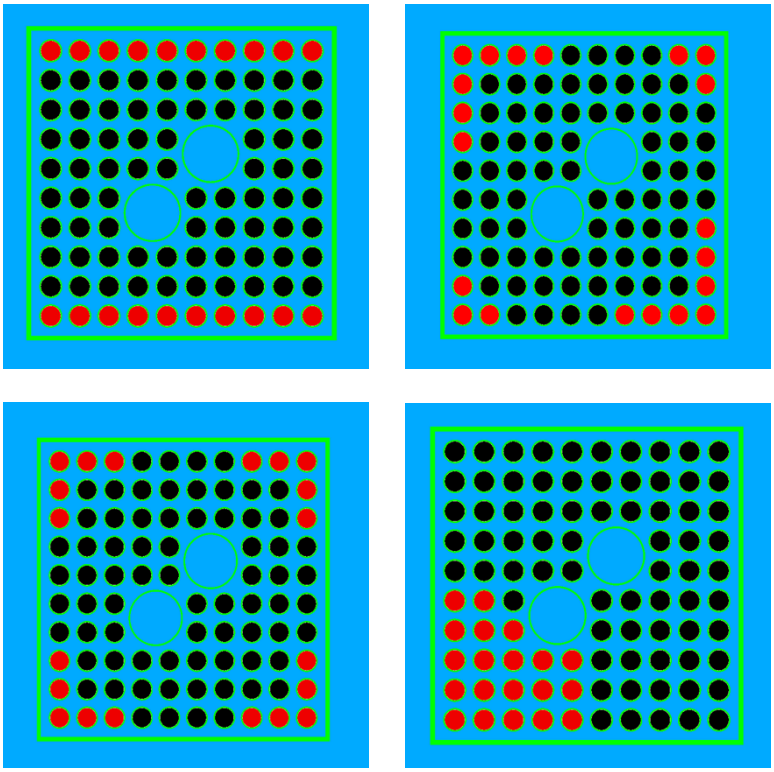

**Figure 3-6. Gadolinium bearing rod (red) placement in a BWR assembly. Listed clockwise; Edge, Corner Oblong, Cluster, Corner.**

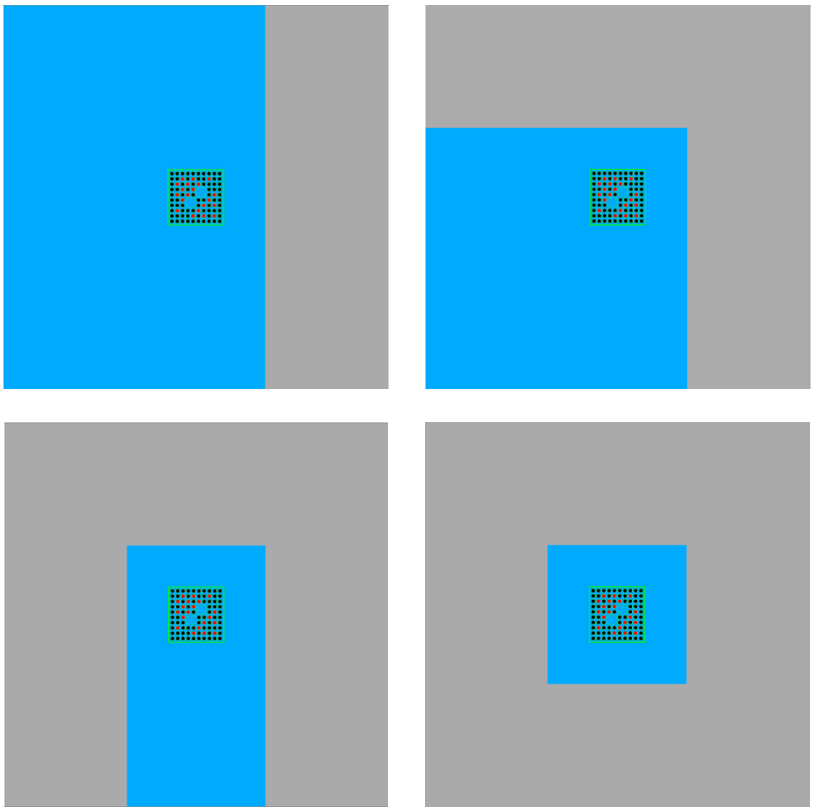

**Figure 3-7. Concrete (grey) reflection on four sides of a BWR assembly.**

# 4. RESULTS AND DISCUSSION

## 4.1 CASE I: SINGLE-ASSEMBLY SCOPING STUDY

The cases shown in Table 1 were run using the CSAS5 sequence of the SCALE 6.3.1 code package with ENDF/B-VII.1 continuous energy cross sections. The regulatory limit for $k_{eff}$ supplied in 10 CFR 50.68 [1] is 0.95, including bias and bias uncertainty. For the results presented herein, a 1% $k_{eff}$ margin was applied to the 0.95 limit to account for the biases and uncertainties, resulting in a target $k_{eff}$ value of 0.94.

Figure 4-1 shows the results of the PWR assembly at different IFBA loadings for the 10 wt % $^{235}U$ fuel. All the results show that the 0.94 $k_{eff}$ target was met without adding $Gd_2O_3$ rods. This is mainly driven by the geometry studied and the increase in IFBA rods.

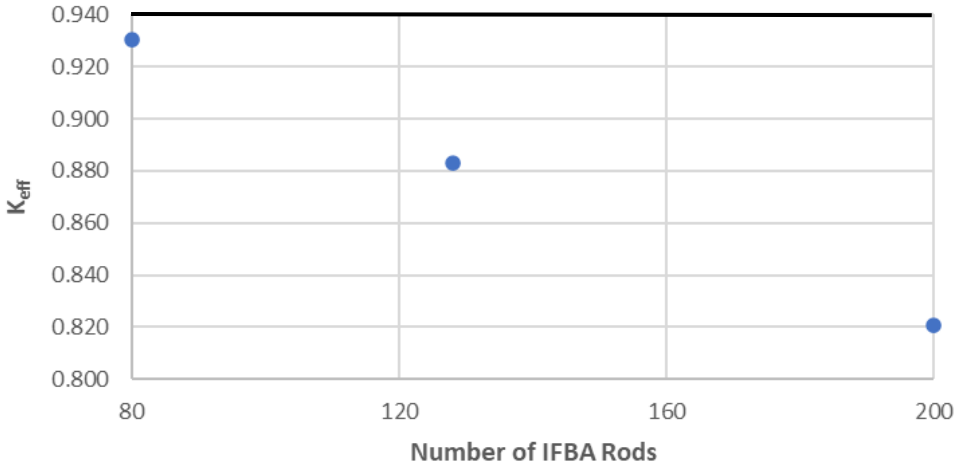


**Figure 4-1. $k_{eff}$ at different IFBA loadings for a PWR assembly at 10 wt % $^{235}$U.**

Figure 4-2 and Figure 4-3 show the results obtained for the PWR assembly at different IFBA loading patterns and gadolinium loadings for the 15 and 20 wt % $^{235}$U fuels, respectively. The 0.94 $k_{eff}$ limit is also shown. Not all cases require the use of gadolinium and IFBA, thus the incomplete appearance. Once a data set reached a value below 0.94, no further $Gd_2O_3$ was added.

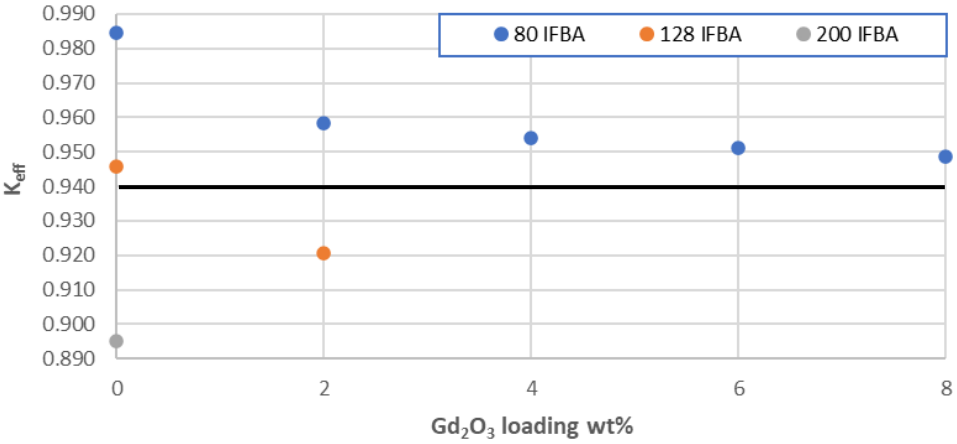


**Figure 4-2. $k_{eff}$ at different IFBA loading patterns and gadolinium loadings for a PWR assembly at 15 wt % $^{235}$U.**

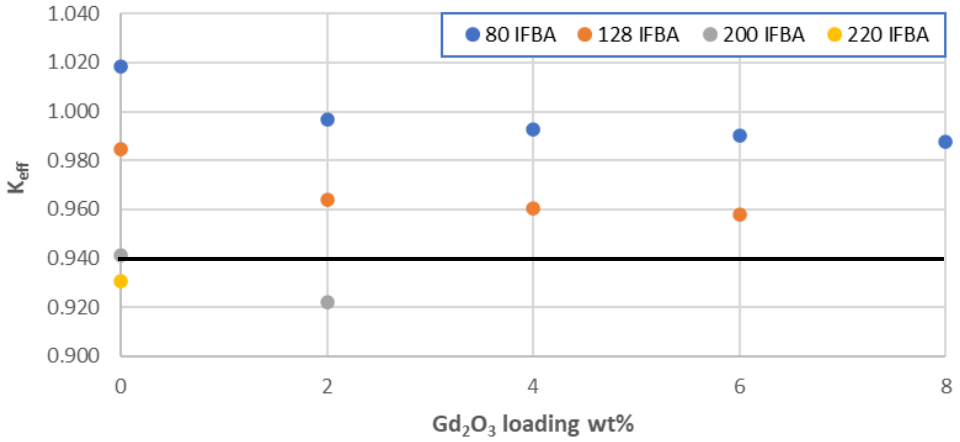


**Figure 4-3. $k_{eff}$ at different IFBA loading patterns and gadolinium loadings for a PWR assembly at 20 wt % $^{235}$U.**

For $^{235}$U rods enriched to 15 wt %, 200 IFBA loading was required to maintain a $k_{eff}$ below 0.94 without adding Gd rods. For the 80 and 128 IFBA loadings, 12 Gd rods with varying wt % were placed in the array to further reduce reactivity. The Gd rods had an initial loading of 2 wt % $Gd_2O_3$ which was increased incrementally by 2 wt % until $k_{eff}$ fell below 0.94 or a maximum loading of 8 wt % was reached. For the lattice with 80 IFBA, the Gd loading was increased until 8 wt % was reached, and $k_{eff}$ was still higher than 0.94. For the lattice with 128 IFBA, the initial 2 wt % Gd loading was sufficient to meet the 0.94 target and required no increase in Gd loading.

For 20 wt % rods, 80, 128, and 200 IFBA loading patterns failed to meet the 0.94 $k_{eff}$ target. The 220 IFBA pattern shown in Figure 3-1 was found to be sufficient to meet the 0.94 target. In addition, the addition of Gd rods was analyzed for the 80, 128, and 200 IFBA loading patterns. Adding 12 Gd rods at 8 wt % was insufficient to bring $k_{eff}$ below 0.94 for the 80 and 128 IFBA patterns. The addition of 12 Gd rods at 2 wt % was sufficient for the 200 IFBA case.

To demonstrate single-assembly reactivity below the 0.94 $k_{eff}$ target, a high number of IFBA rods is needed in the 15–20 wt % range, or the IFBA should be supplemented with Gd rods.

Figure 4-4 shows the results for the BWR assembly at different fuel enrichments and gadolinium loadings. All the results show a significant margin to the $k_{eff}$ limit. As expected, the increase in $^{235}$U enrichment results in higher $k_{eff}$ values, and the increase in Gd loading results in lower $k_{eff}$ values. The isolation from other assemblies provided by 40 cm of water surrounding the assembly, as well as the high number of Gd rods (20), ensure that $k_{eff}$ remains low.

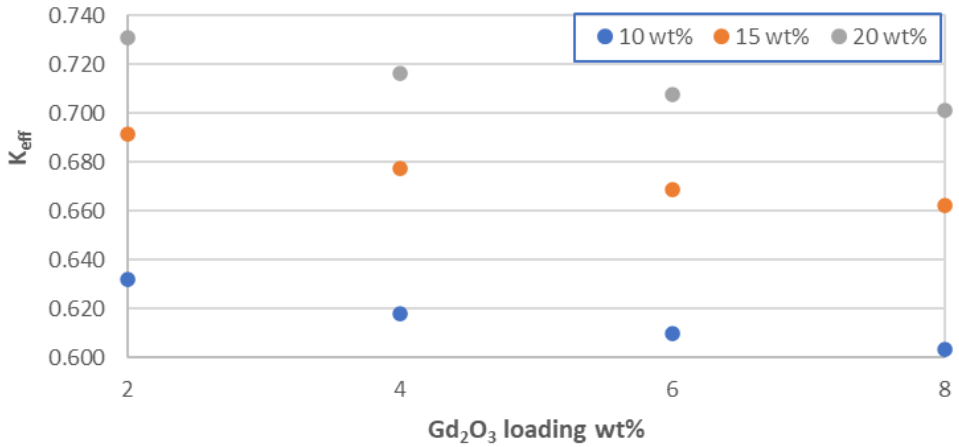


**Figure 4-4. $k_{eff}$ at different fuel enrichments and gadolinium loadings for a BWR assembly with 20 gadolinium bearing rods.**

The results for PWRs are summarized in the upper two tables of Figure 4-5, and BWR results are summarized in the bottom table. These results show that increasing burnable absorber can sufficiently offset increased enrichments. For the PWR cases with gadolinium, the extra Gd does provide reactivity suppression, but the predominant effect is caused by the initial introduction of the 12 Gd-bearing rods, not the increase in weight percent following their introduction, which has rapidly diminishing returns. Thus, the second table only includes conditions with 12 2 wt% Gd rods, demonstrating the additional conditions that meet the 0.94 requirement for 15 and 20 wt%.

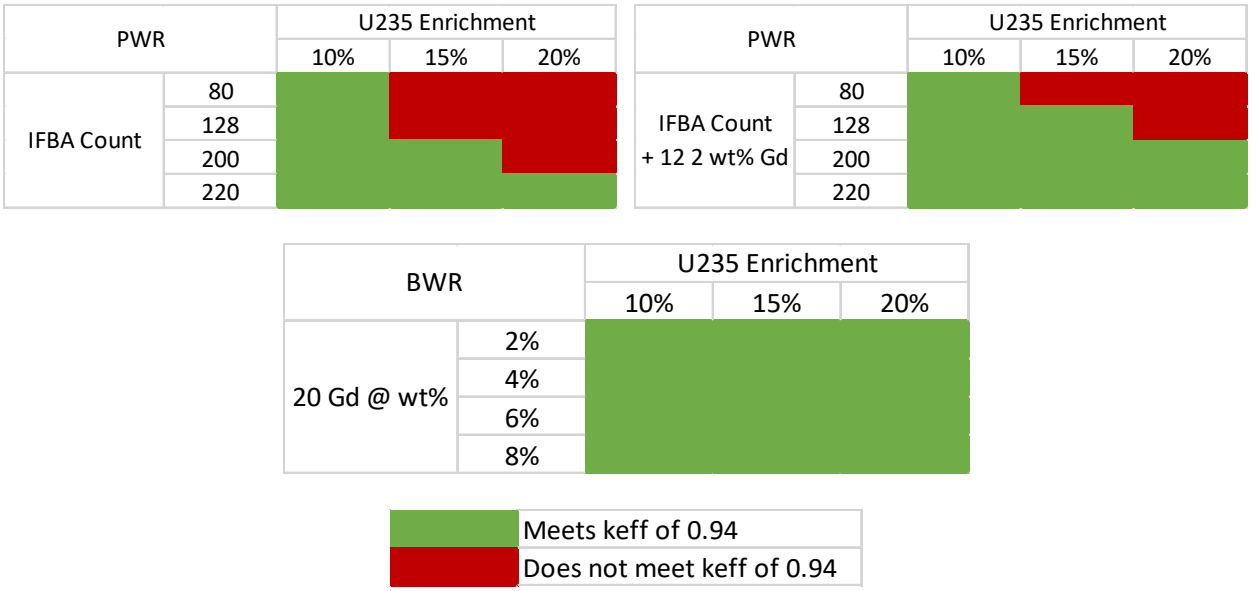


**Figure 4-5. Summary of burnable absorber and fuel enrichment requirements for Case I.**

## 4.2 CASE II: SINGLE-ASSEMBLY FULL STUDY

As noted in Section 2.2, the model changes that were made to address ATF fuels are the addition of a 20 µm coating of chromium on the cladding and the addition of a 1,000 ppm $Cr_2O_3$ dopant with an increased

density. These changes are not illustrated because neither is particularly predisposed to visualization because dopant is homogenously distributed, and the cladding layer is very thin. Results are given in Table **4**. Figure 4-6 plots the Cr coating's $k_{eff}$ differential for PWRs, where $\Delta k_{eff}$ is the eigenvalue determined in Case I subtracted from the eigenvalue determined by the ATF study: $k_{ATF}$ - $k$. A more reactive configuration with ATF would be positive, and a less reactive configuration with ATF would be negative.

**Table 4. Calculated $k_{eff}$ for ATF concepts**

| **20 µm Cr coating** | | | | **1,000 ppm $Cr_2O_3$ dopant** | | | |
|---|---|---|---|---|---|---|---|
| **PWR** | 10% | 15% | 20% | **PWR** | 10% | 15% | 20% |
| 80 IFBA | 0.927 | 0.981 | 1.015 | 80 IFBA | 0.933 | 0.987 | 1.020 |
| 128 IFBA | 0.880 | 0.943 | 0.982 | 128 IFBA | 0.886 | 0.948 | 0.988 |
| 200 IFBA | 0.818 | 0.892 | 0.939 | 200 IFBA | 0.825 | 0.898 | 0.944 |
| **BWR** | 10% | 15% | 20% | **BWR** | 10% | 15% | 20% |
| 20 8 wt% Gd | 0.601 | 0.660 | 0.699 | 20 8 wt% Gd | 0.606 | 0.665 | 0.704 |

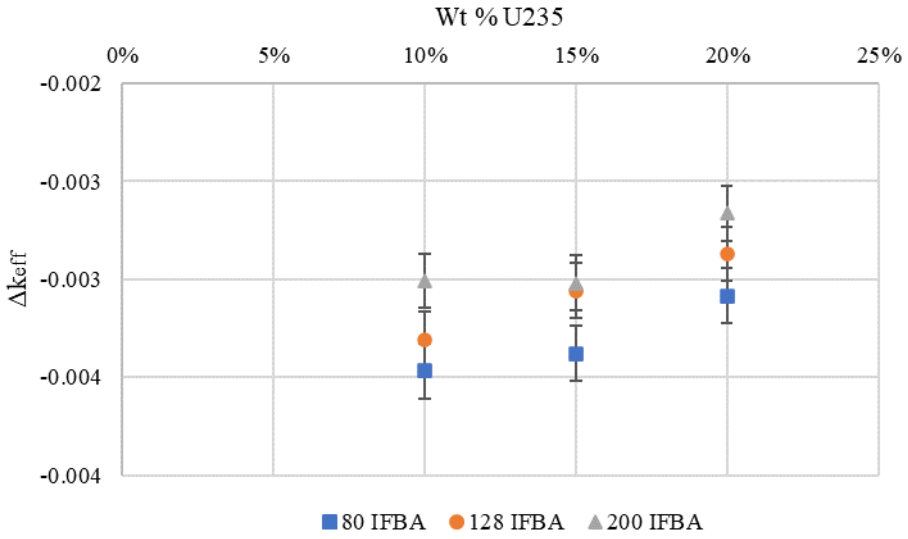


**Figure 4-6. $k_{eff}$ differential for Cr-Coated PWR fuel by IFBA and enrichment.**

Although the initial inspection appears to show a slight trend with enrichment and IFBA loading, the behavior is largely statistical noise. In all cases, the additional coating has a negative reactivity effect with a reduction ranging between 266 and 347 pcm in Figure 4-7. BWRs show a similar behavior with a lower magnitude reduction of 180–200 pcm. It is expected that a thin layer of chromium would result in a reactivity penalty.

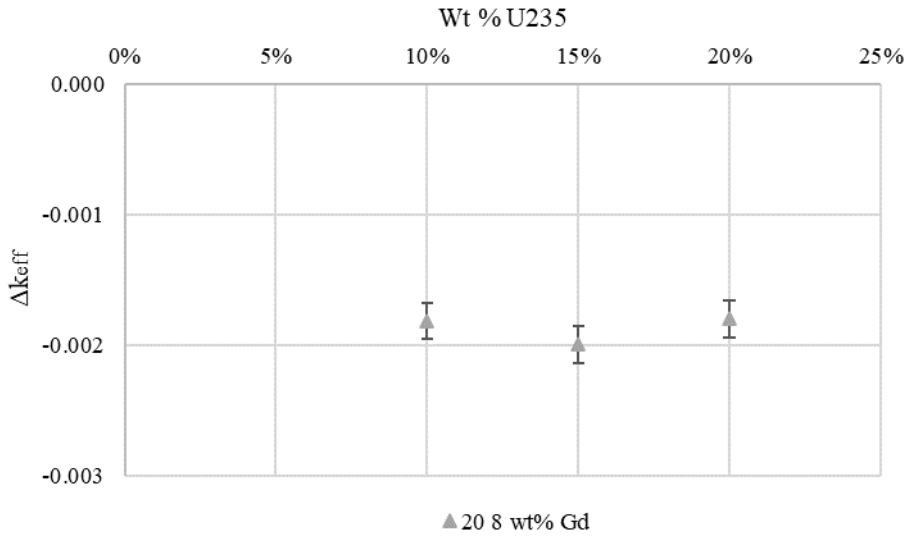


**Figure 4-7. $k_{eff}$ differential for Cr-Coated BWR fuel.**

Figure 4-8 plots the $Cr_2O_3$ dopant $k_{eff}$ differential for PWRs. With an increased fuel density and identical fuel rod size, more fuel was introduced, offsetting reductions from the 1,000 ppm $Cr_2O_3$ of dopant replacing fuel. While the most variation is 100 pcm between 10 and 20 wt% or between 80 and 200 IFBA, there is a trend of a lessened increase in reactivity as a result of the dopant and an increased density with both enrichment and IFBA. This is likely a plateauing effect of the increased fissile material per assembly, whether caused by increased density or enrichment. In all cases, the additional coating is a positive reactivity effect, with an increase ranging between a 218 and 384 pcm. Figure 4-9 displays results for BWRs in which no trend on enrichment is evident. An increase in reactivity is seen, but it is very consistent, between 246 and 254 pcm, with increasing enrichment. It is expected that a dopant of chromium would result in a reactivity increase as a result of increased fuel density.

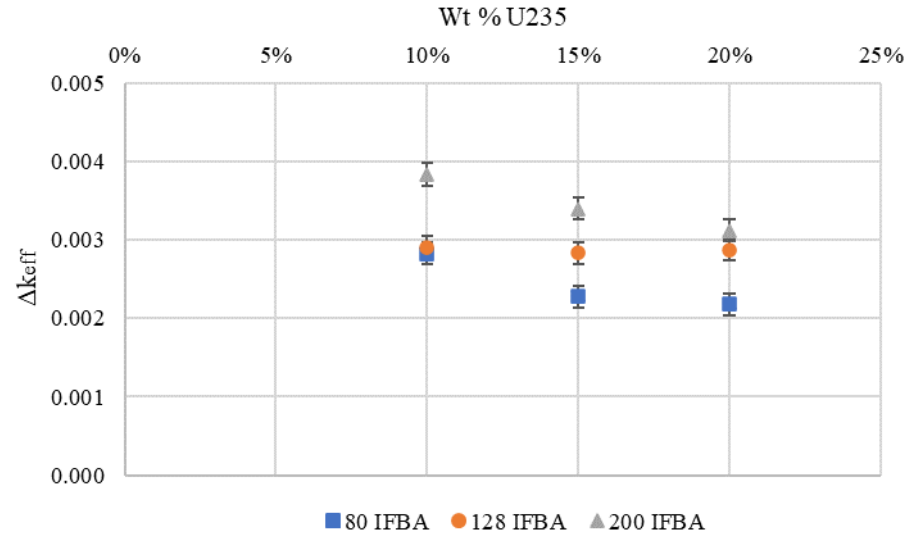


**Figure 4-8. $k_{eff}$ differential for $Cr_2O_3$-doped PWR fuel by IFBA and enrichment.**

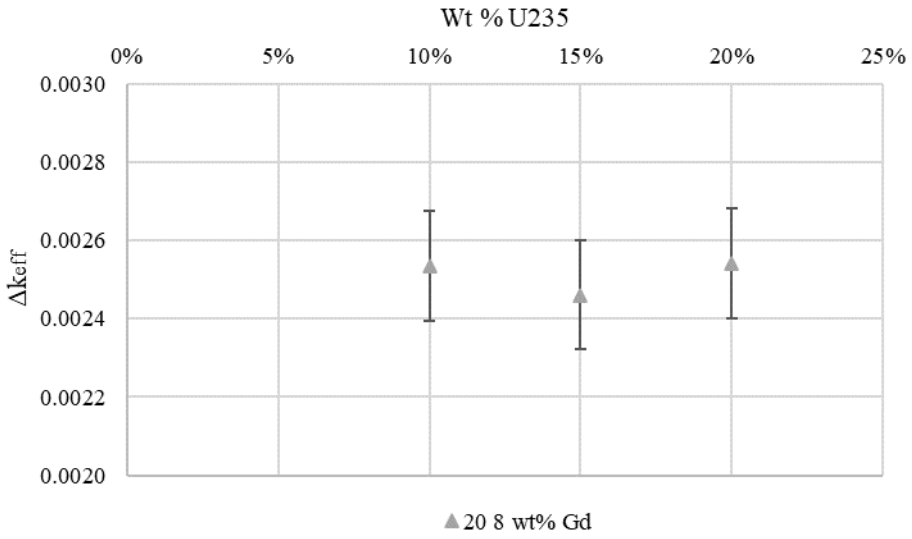


**Figure 4-9. $k_{eff}$ differential for $Cr_2O_3$-doped BWR fuel.**

The sensitivity of Gd-doped locations in the BWR lattice was investigated. Lattice patterns are provided in Section 3. The $k_{eff}$ values are shown in Table 5, and they vary up to 6% based on whether the gadolinium was centrally or peripherally placed. The number of gadolinium rods was conserved.

**Table 5. Calculated $k_{eff}$ for BWR gadolinium rod placement**

| Configuration | Corner | Edge | Corner Oblong | Cluster |
|---|---|---|---|---|
| Keff | 0.672 | 0.669 | 0.671 | 0.726 |

PWR annular fuel blankets were substituted for the lower 8 inches of fuel, with fuel 2 wt% $^{235}U$ less than nominal in an annular blanket at the top and bottom of the fuel rod. For fresh fuel, as examined, no depletion effects are present. The central high fission density region of the assembly is not depleted but is fresh. The fission density driving the eigenvalue is therefore minimally impacted by this peripheral replacement and removal of fuel. Only the PWR assembly with 200 IFBA was examined. The result of this annular blanket analysis is shown in Table **6**. The effect is a 23 to 30 pcm reduction in $k_{eff}$ relative to the results presented in Section 4.1. This is a statistically insignificant effect for the considered enrichment, blanket size, and annulus.

**Table 6. Calculated $k_{eff}$ for PWR annular blanket**

| Annular blanket | 10% | 15% | 20% |
|---|---|---|---|
| 200 IFBA | 0.821 | 0.895 | 0.941 |

For concrete reflection, 128 IFBA for PWR lattices was used, whereas of 20 Gd rods at 8 wt% were for BWRs. Based on the initial results in Section 4.1, PWRs with 128 IFBA are below 0.94 at 10 wt%, but they are above 0.94 for 15 and 20 wt%. BWRs with 20 8 wt% Gd are below 0.94 at all enrichments. The minor reactivity increase for these statepoints is insufficient to increase BWRs or the 10 wt% PWR assembly above 0.94. Figure 4-10 and Figure 4-11 show the relative increases in reactivity for PWRs and BWRs, with increasing concrete reflection. The effect ranges from 44 to 232 pcm, increasing with additional concrete. Higher enrichments also have a slightly higher effects.

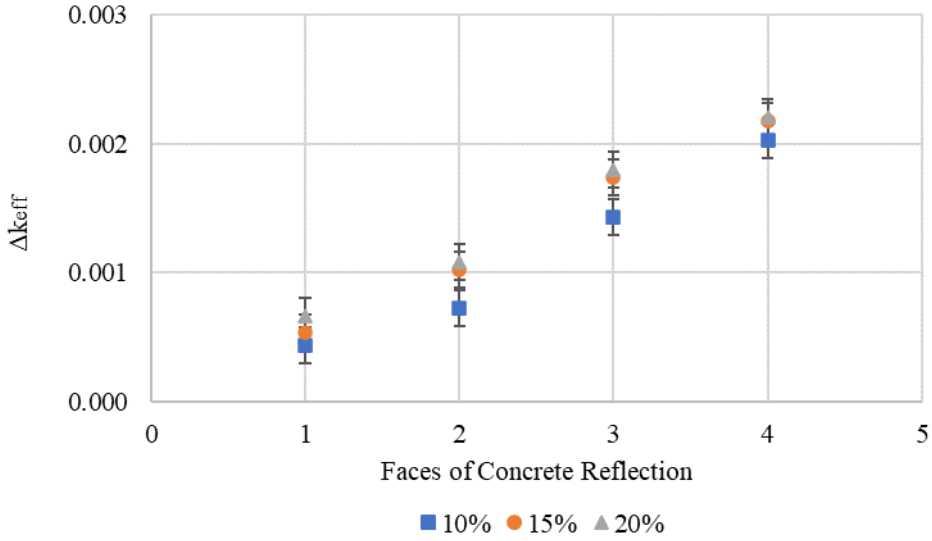


**Figure 4-10. $k_{eff}$ differential for PWR concrete reflection.**

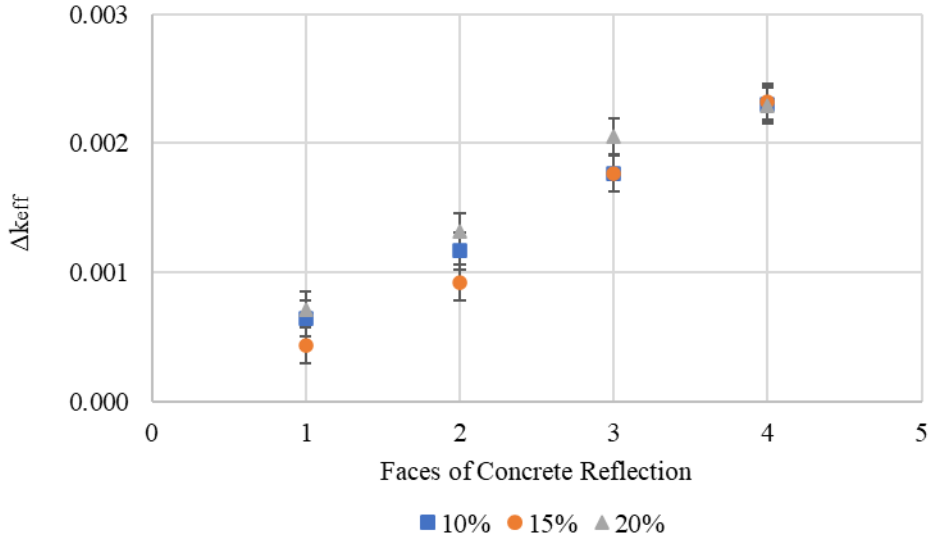


**Figure 4-11. $k_{eff}$ differential for BWR concrete reflection.**

# 5. CONCLUSIONS

In response to requests for assemblies with increased enrichment, this study was implemented to determine the required burnable absorbers as a function of enrichment. Both PWR and BWR assemblies were studied, and operational conditions specific to each were also examined. Two studies were performed: (1) an initial scoping study of the needed burnable absorber, and (2) a follow-up study on the magnitude of operational conditions that may occur or that should be considered. Both studies examined BWR and PWR assemblies.

The results of the first study concern the specific request for information on how increased enrichment can be offset by burnable absorbers, namely IFBA and Gd rods. Historically, IFBA is preferentially used in PWRs, and Gd is used in BWRs. For PWRs, several IFBA patterns were taken from recent work to determine how 10, 15, and 20 wt% $^{235}U$ fuel would respond. For BWRs, the same pattern of 20 Gd rods was used at varying concentrations of gadolinium. Figure 4-5 provides a summary of both PWR and BWR behavior in Case I, indicating that increased enrichment can be offset with increased absorber loading.

For 10 wt% fuel, 80 or more IFBA was shown to maintain a $k_{eff}$ below 0.94, a limit devised to meet the 10 CFR 50.68 regulatory limit of 0.95 while accounting for nuclear data and code biases. For 15 wt% fuel, 80 IFBA alone was shown to be insufficient, as was 128 IFBA. However, 200 IFBA or greater, or 128 IFBA and 12 Gd rods at 2 wt%, were shown to be sufficient. For 20 wt%, 220 or more IFBA are sufficient, as is 200 IFBA with 12 Gd rods at 2 wt%. For BWRs, the use of 20 Gd rods at any weight percent was sufficient to keep the individual assembly below a $k_{eff}$ of 0.94. The maximum $k_{eff}$ of such cases is 0.731, which is well below the 0.94 limit. This is a result of the smaller BWR assembly with 22% of rods (20 of 92) containing a homogenously distributed strong neutron absorber at a weight fraction of at least 2 wt%.

The second study was performed to address more subtle minor differences. The magnitude of all studies other than the gadolinium location study was within several hundred pcm of the nominal values. Substituting 8 inches of the PWR rod ends with a less enriched annular design resulted in a decrease in eigenvalue of less than a 30 pcm. This is because annular blankets become more impactful with depletion as the fission density redistributes, and the fuel involved in this study is fresh. The analysis of partial length rods in BWRs resulted in a maximum decrease of 123 pcm. The addition of concrete reflectors on each face of the BWR and PWR assemblies resulted in steady increases in reactivity, with a maximum of 232 and 221 pcm respectively, for four faces of concrete reflection. The use of $Cr_2O_3$ dopant was shown to increase fuel density while introducing slight absorption, thus resulting in 218–384 pcm increases in reactivity, depending on fuel type and enrichment. The introduction of Cr-coated cladding added absorption alone and reduced $k_{eff}$ by 180–347 pcm, depending on fuel type and enrichment. Ignoring direction, all these effects in magnitude are summed to one percent or less in $k_{eff}$, even when the direction of the effect is ignored. These changes are in the range that can be addressed by the existing margin to 0.94 for the cases shown in Figure 4-5. The positioning of Gd rods is much more sensitive, resulting in changes of up to 6 % in $k_{eff}$. Although these cases are not realistic, they demonstrate the value of the Gd in the assembly: the positioning of Gd has a magnitude of effect similar to that of a 5 wt% increase in enrichment. The examined Gd repositionings have a negative rather than a positive effect on reactivity, and combined with the lower single assembly reactivity of BWR assemblies, $k_{eff}$ remains well subcritical.

## 6. REFERENCES


1. United States Code of Federal Regulations, Title 50, Energy, Part 68—Criticality Accident Requirements, No. 10CFR50 (2006).
2. Shaw, A. M., Clarity, J. B. 2022. *Impacts of LEU+ and ATF on Fresh Fuel Storage Criticality Safety,* ORNL/TM-2021/2330, Oak Ridge National Laboratory, Oak Ridge, Tennessee.
3. General Electric Systems Technology Manual, Chapter 2.2, Fuel and Control Rods System, Nuclear Regulatory Commission, ADAMS ML11258A302.
4. M. A. Hannah, Axial Fuel Blanket Design and Demonstration, First Semi-Annual Progress Report: January-September 1980, DOE/ET/34020-1, Babcock & Wilcox, Lynchburg, VA, (1980).
5. Hall, R., et al. 2021. *Extended-Enrichment Accident-Tolerant LWR Fuel Isotopic and Lattice Parameter Trends.* ORNL/TM-2021/1961. Oak Ridge: Oak Ridge National Laboratory.
6. Arborelius, J., et al. 2006. *Advanced Doped UO2 Pellets in LWR Applications*. Journal of Nuclear Science and Technology, 43:9, 967-976, DOI: 10.1080/18811248.2006.9711184
7. Silva, C. M., Hunt, R. D., Holliday, K. S. 2021. "An Evaluation of Tri-Valent Oxide ($Cr_2O_3$) as a Grain Enlarging Dopant for $UO_2$ Nuclear Fuels Fabricated Under Reducing Environment," *Journal of Nuclear Materials*, Vol. 553, https://doi.org/10.1016/j.jnucmat.2021.153053.
8. Fensin, M. L. 2004. *Optimum Boiling Water Reactor Fuel Design Strategies to Enhance Reactor Shutdown by the Standby Liquid Control System*, Master of Engineering Thesis, University of Florida.
9. Mertyurek, U., Bae, J. W., Hu, J., Wieselquist, W. A. 2022. *Assessment of Core Physics Characteristics of Extended Enrichment and Higher Burnup LWR Fuels using the Polaris/PARCS Two-Step Approach Vol. II: BWR Fuel*, ORNL/TM-2022/2444, Oak Ridge National Laboratory, Oak Ridge, Tennessee.
10. Wieselquist, W. A. and Lefebvre, R. A., Eds. 2023. *SCALE 6.3.1 User Manual*. ORNL/TM-SCALE-6.3.1, Oak Ridge National Laboratory, Oak Ridge, Tennessee.
11. Westinghouse *AP1000 Design Control Document* https://www.nrc.gov/docs/ML1117/ML11171A431.pdf
12. Westinghouse *Technology Systems Manual* https://www.nrc.gov/docs/ML1122/ML11223A338.pdf
13. Chadwick, M. B., et al., 2011. "ENDF/B-VII.1 Nuclear Data for Science and Technology: Cross Sections, Covariances, Fission Product Yields and Decay Data," *Nuclear Data Sheets*, 112, pp. 2887–2996.
14. Hu, J., Mertyurek, U., and Wieselquist, W. A. 2022. *Assessment of Core Physics Characteristics of Extended Enrichment and Higher Burnup LWR Fuels using the Polaris/PARCS Two-Step Approach. Vol. I: PWR Fuel*. ORNL/TM-2022/1831, Oak Ridge National Laboratory, Oak Ridge, Tennessee.
15. Godfrey, A. 2011. *VERA Core Physics Benchmark Progression Problem Specifications, Revision 4*, CASL Technical Report: CASL-U-2012-0131-004.

# APPENDIX A. Sample CSAS5 Input Files

**BWR, 15 wt %: 20 Gd rods @ 4 wt %**

```
=csas5 parm=(   )
BWR single assembly, 15 wt %, 20 Gd (4 wt %)
ce_v7.1
‘References: 1- ORNL/TM-2022/2444
read parameters

     sig=0.0001 gen=10150 npg=15000 nsk=150 htm=no

end parameters
read comp
‘15 wt % fuel
uo2 1 den=10.550 1.0 293.0
      92235 15
      92238 85 end
‘cladding
zirc2 2  1.0  end
‘mod/reflector
water 3  1.0  end
‘15 wt % fuel w/ 4 wt % Gd
uo2 5 den=10.55 0.96 293 92235 15 92238 85 end
gd2o3 5 den=10.55 0.04  end
end comp
read geometry

‘Fuel Rod [1]
unit 1
  zcylinder 1 1 0.438 381 0.0
  zcylinder 0 1 0.447 381 0.0
  zcylinder 2 1 0.513 381 0.0
  cuboid    3 1 4p0.6475 381 0.0

‘Gad Fuel Rod [1]
unit 2
  zcylinder 5 1 0.438 381 0.0
  zcylinder 0 1 0.447 381 0.0
  zcylinder 2 1 0.513 381 0.0
  cuboid    3 1 4p0.6475 381 0.0

’10 × 10 assembly [1]
global unit 3
  array   1    -6.475 -6.475 0
cuboid 3 1 4p6.703 381 0
hole 5 1.295 1.295 0
hole 5 -1.295 -1.295 0
hole 6 2.59 -6.475  0
hole 7 -2.59 -6.475  0
hole 8 -2.59 0  0
hole 9 0 -6.475  0
hole 10 0 2.59  0
cuboid 2 1 4p6.9062 381 0
replicate 3 1 6*40 1

‘water tube hole [1]
unit 5
zcylinder 3 1 1.2 381 0
zcylinder 2 1 1.28 381 0

unit 6
  array   2    0 0 0
unit 7
  array   3    0 0 0
unit 8
  array   4    0 0 0
unit 9
  array   5    0 0 0
unit 10
  array   6    0 0 0
end geometry

read array
  ara=1
‘array of fuel rods [1]
  nux=3   nuy=10   nuz=1
fill
1 1 1
1 1 1
1 2 1
1 1 1
1 1 2
1 2 1
1 1 2
1 2 1
1 1 2
1 1 1
end fill

  ara=2
‘array of fuel rods [1]
  nux=3   nuy=10   nuz=1
fill
1 1 1
1 2 1
1 1 1
1 2 1
2 1 1
1 2 1
1 1 1
1 1 1
2 1 1
1 1 1
end fill

  ara=3
‘array of fuel rods [1]
  nux=2   nuy=3   nuz=1
fill
1 1
1 2
1 1
end fill
  ara=4
‘array of fuel rods [1]
  nux=2   nuy=5   nuz=1
fill
2 1
1 2
2 1
1 2
1 1
end fill

  ara=5
‘array of fuel rods [1]
  nux=2   nuy=5   nuz=1
fill
1 1
1 2
2 1
1 2
1 1
end fill

  ara=6
‘array of fuel rods [1]
  nux=2   nuy=3   nuz=1
fill
2 1
1 1
1 1
end fill

end array
read bounds
‘reflective boundary conditions
all=mirror
end bounds
end data
end
```

## PWR, 15 wt %: 128 IFBA

```
=csas5 parm=(   )

PWR single assembly, 15 wt %, 128 IFBA 2× (3.137 mgB10/in)

ce_v7.1

‘References: 1- ORNL/TM-2022/1831

read parameters

     sig=0.0001 gen=10150 npg=15000 nsk=150 htm=no



end parameters

read comp

‘10 wt % fuel [1]

uo2 1 den=10.376 1.0 293.0

       92235 15

       92238 85 end

‘cladding

zirc4 2  1.0  end

‘mod/reflector

water 3  1.0  end

‘IFBA 3.137 mg/inch [1], loading adjusted by thickness

atomzrb2 4 3.85 2 40000 1 5000 2 1.0 293 5010 50 5011 50 end

end comp

read geometry

‘Fuel Rod [1]

unit 1

  zcylinder 1 1 0.4096 365.76 0.0

  zcylinder 0 1 0.418 365.76 0.0

  zcylinder 2 1 0.475 365.76 0.0

  cuboid    3 1 4p0.63 365.76 0.0



‘Instrument and Guide Tube

unit 2

  zcylinder 3 1 0.5715 365.76 0.0

  zcylinder 2 1 0.61214 365.76 0.0

  cuboid    3 1 4p0.63 365.76 0.0



‘IFBA Fuel Rod [1]; 10 um mult. By 2/1.5

unit 3

zcylinder 1 1 0.4096 365.76 0.0

  zcylinder 4 1 0.41093 365.76 0.0

  zcylinder 0 1 0.418 365.76 0.0

  zcylinder 2 1 0.475 365.76 0.0

  cuboid    3 1 4p0.63 365.76 0.0



‘17 × 17 assembly

global unit 4

  array   1    -10.71 -10.71 0

'40 cm water reflector

replicate 3 1 6*40 1



end geometry



read array

  ara=1

'array of fuel rods [1]

   nux=17   nuy=17   nuz=1

fill

3 1 1 1 3 1 1 3  1  3 1 1 3 1 1 1 3

1 1 3 1 1 3 1 1  3  1 1 3 1 1 3 1 1

1 3 1 3 3 2 3 3  2  3 3 2 3 3 1 3 1

1 1 3 2 3 3 1 1  3  1 1 3 3 2 3 1 1

3 1 3 3 1 3 1 1  3  1 1 3 1 3 3 1 3

1 3 2 3 3 2 3 3  2  3 3 2 3 3 2 3 1

1 1 3 1 1 3 1 1  3  1 1 3 1 1 3 1 1

3 1 3 1 1 3 1 1  3  1 1 3 1 1 3 1 3

1 3 2 3 3 2 3 3  2  3 3 2 3 3 2 3 1

3 1 3 1 1 3 1 1  3  1 1 3 1 1 3 1 3

1 1 3 1 1 3 1 1  3  1 1 3 1 1 3 1 1

1 3 2 3 3 2 3 3  2  3 3 2 3 3 2 3 1

3 1 3 3 1 3 1 1  3  1 1 3 1 3 3 1 3

1 1 3 2 3 3 1 1  3  1 1 3 3 2 3 1 1

1 3 1 3 3 2 3 3  2  3 3 2 3 3 1 3 1

1 1 3 1 1 3 1 1  3  1 1 3 1 1 3 1 1

3 1 1 1 3 1 1 3  1  3 1 1 3 1 1 1 3

end fill

end array

read bounds

'reflective boundary conditions

all=mirror

end bounds

end data

end
```